International J. of Math. Sci. & Engg. Appls. (IJMSEA)
ISSN 0973-9424, Vol. 9 No. III (September, 2015), pp. 197-210

COMPLEX DYNAMICS AND CHAOS CONTROL IN DUFFING-VAN DER POL EQUATION WITH TWO EXTERNAL PERIODIC FORCING TERMS

YANXIANG SHI
School of Mathematical Sciences,
Shanxi University, 030006, China

Abstract

Duffing-Van der Pol equation with fifth nonlinear-restoring force and two external periodic forcing terms is investigated. By applying numerical simulations, including phase portraits, potential diagram, Poin*cáre* maps, bifurcation diagrams and maximal Lyapunov exponents, the nonlinear behavior and the complex dynamics of the system with two external periodic excitations are analyzed. At last, two kinds of methods are applied to control the chaotic behaviors of the system, effectively to a steady periodic orbit (or quasi-periodic orbit).

1. Introduction

Chaos is a modern subject with rich academic background of deep non-linear physics and mathematics content, and a large number of non-linear systems may appear chaotic phenomena and chaos control is a hot topic in control science.

Key Words : *Dynamics, Duffing-Van der Pol equation, Chaos, Chaos control.*

In this paper we consider the Duffing-Van der Pol equation with fifth nonlinear-restoring force and two external periodic forcing terms

$$\ddot{x} - \mu(1 - x^2)\dot{x} + \omega_0^2 x + \lambda x^3 + \beta x^5 = f_1 \cos \omega_1 t + f_2 \cos \omega_2 t. \tag{1}$$

The equivalent system of the system (1) can be written as

$$\begin{cases} \dot{x} = y, \\ \dot{y} = \mu(1 - x^2)y - \omega_0^2 x - \lambda x^3 - \beta x^5 + f_1 \cos \omega_1 t + f_2 \cos \omega_2 t, \end{cases} \tag{2}$$

where $\mu, \omega_0, \lambda, \beta, f_j$ and ω_j $(j = 1, 2)$ are real parameters; $\mu(1-x^2)\dot{x}$ can be regarded as dissipation or damping term, μ is damping coefficient; $f_j \cos \omega_j t$ $(j = 1, 2)$ are periodic forcings, f_j and ω_j $(j = 1, 2)$ can be regarded as the amplitudes and the frequencies of the forcings respectively. It is taken as $\mu = 0.1, \omega_0^2 = 1, \lambda = -3$ and $\beta = 2$ in the system (2).

The system (2) is equivalent to the combination of the Duffing oscillator and the Van der Pol oscillator, and both are non-linear oscillator with wide range of applications. The system (2) can be used to describe the structure of flow-induced vibration of a simple model [10], and to simulate the optical bistability in one type of dispersive media [4]. Duffing oscillator $\big(\mu = 0$ in the system (1) or (2)$\big)$ and the Van der Pol oscillator $\big(\lambda = 0$ and $\beta = 0$ in the system (1) or (2)$\big)$ have an important application background in nonlinear systems. In $[3, 7, 9, 13, 16, 19 - 22]$, the interesting structure of bifurcation sets, bifurcation roads, the chaotic dynamics and the phenomenon of phase-locked are found. The study of stochastic Duffing-Van der pol system without external forcing terms can be found in $[11, 17]$ and the bifurcation behavior, the function of probability distribution and the stochastic behavior are discussed. Periodically excited Duffing-Van der Pol oscillator is a typical nonlinear vibration system and has rich dynamic behavior. The bifurcation structure, chaos behavior and chaos control of the system (2) when $\beta = 0$ are found in $[1, 14, 15, 18]$. Jing Z.J. etc. studied the complex dynamic behavior of the system (2) in [8]: the criterion of existence of chaos under the periodic perturbation is given by using Melnikov's method; By using second-order averaging method and Melnikov method, the authors gave the criterion of existence of chaos in averaged systems under quasi-periodic perturbation. They also gave numerical simulations to support the theoretical results obtained in the precious section and to find other new dynamics. Furthermore, the study of chaos control (from chaotic to periodic) and chaos

anti-control (from periodic to chaotic) are interesting. More importantly within the biological and electronic context, chaos control and chaos anti-control show great potential for future applications. Chaos control of chaotic pendulum system is shown in [12]. Ge Z.M. and Leu W.Y. studied the chaos anti-control and synchronization of a two-degrees-of-freedom loudspeaker system in [5]. The chaos control for Duffing-Van der Pol system with one external periodical forcing term and cubic nonlinear-restoring force is studied in [2, 6]. However, there are few works on the chaos control of the system (2) in the current domestic and international literature, it is necessary to research further in this area.

Motivated by the findings in [2, 6, 8], in this paper, the system (2) is analyzed and simulated in detail by numerical simulations. By using phase portraits, potential diagram, Poin*cáre* maps, bifurcation diagrams and maximal Lyapunov exponents, the dynamical characteristics of the system (2) with the changes of the bifurcation parameters are reflected intuitively, then the effect of bifurcation parameters on dynamical characteristics is obtained and it is proved that the system (2) exists chaos indeed. Finally, the chaos of the system (2) is controlled to stable periodic orbits (or quasi-periodic orbits) by two kinds of control methods.

The paper is organized as follows. In Section 2, we briefly describe the fixed points and phase portrait for the unperturbed system of Eq. (2). Furthermore, the chaos of the system (2) is given, corresponding to amplitude f_1 and frequency ω_1. The chaos of the system (2) in Section 2 is controlled by two kinds of chaos control methods in Section 3: variable feedback control and coupled feedback control. Conclusions are made in Section 4.

2. The Dynamical Behaviors of the System (2)

2.1 Fixed Points and Phase Portrait for the Unperturbed System

If $\mu = f_j = 0$ $(j = 1, 2)$, the system (2) is considered as an unperturbed system and can be written as

$$\begin{cases} \dot{x} = y, \\ \dot{y} = -\omega_0^2 x - \lambda x^3 - \beta x^5. \end{cases} \tag{3}$$

The system (3) is a Hamiltonian system with Hamiltonian function

$$H(x, y) = \frac{1}{2}y^2 + \frac{1}{2}\omega_0^2 x^2 + \frac{1}{4}\lambda x^4 + \frac{1}{6}\beta x^6,$$

and the function

$$V(x) = \frac{1}{2}\omega_0^2 x^2 + \frac{1}{4}\lambda x^4 + \frac{1}{6}\beta x^6$$

is called the potential function. The systems (3) is a three-well system as the parameter values are taken as $\omega_0^2 = 1, \lambda = -3$ and $\beta = 2$. There are five fixed points: $(0,0), (x_j, 0)$ $(j = 1,2,3,4)$, $x_{1,2} = \pm\sqrt{z_1}$, $x_{3,4} = \pm\sqrt{z_2}$, where $z_{1,2} = \dfrac{-\lambda \pm \sqrt{\lambda^2 - 4\beta\omega_0^2}}{2\beta}$. $C_2(0,0), C_3(x_1,0)$ and $C_1(x_2,0)$ are centers, $S_2(x_3,0)$ and $S_1(x_4,0)$ are saddles.
The phase portrait and potential diagram are shown in Fig. 1(a) and (b), respectively. In Fig. 1(a) the saddle $S_1(x_4,0)$ is connected itself by homoclinic orbits Γ_{hom}^-, the other saddle $S_2(x_3,0)$ is connected itself by homoclinic orbits Γ_{hom}^+, S_1 and S_2 are connected by two heteroclinic orbits $\Gamma_{het}^{\pm}$.

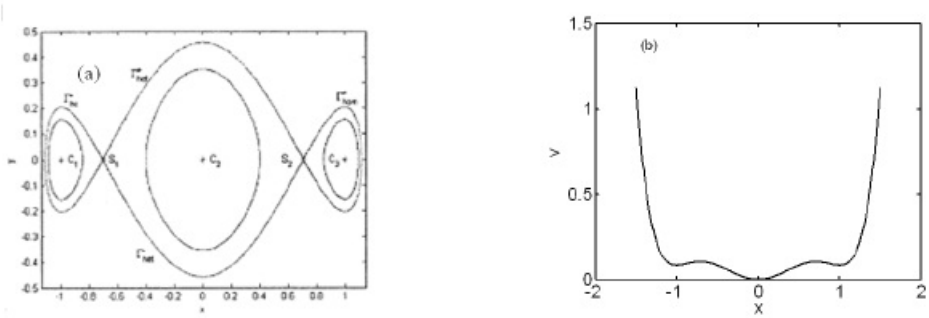

Figure 1: Phase portrait and potential of the unperturbed system (3) for $\omega_0^2 = 1, \lambda = -3, \beta = 2$.

2.2 Chaos of the System (2)

The system (2) is a multi-parameter dynamical system and the stability and global structure will change as parameters change. The qualitative state (for example, a state of equilibrium, or the number of periodic motion and stability, etc.) will be sudden changed and appear bifurcation as the parameters are taken as certain critical values. The dynamical characteristics, complexity and nonlinear characteristics of the system (2) with external periodic excitation, corresponding to f_1 and ω_1 are considered respectively.

Case I : f_1 is bifurcation parameter, and ω_1 is not rational relative to ω_2.
The Poin*cáre* map of the system (2) is shown in Fig. 2 for $f_1 = 6.1, \omega_1 = 1, f_2 = 0.75$ and $\omega_2 = \sqrt{5}$. It can be seen that the system is in chaotic motion from Fig. 2. We

plot the bifurcation diagram of the system (2) in (f_1, x) plane for $\omega_1 = 1, f_2 = 0.75$ and $\omega_2 = \sqrt{5}$ in Fig. 3(a), and the maximal Lyapunov exponents corresponding to Fig. 3(a) are plotted in Fig. 3(b) for confirming the chaotic dynamics. It can be found that there are three different chaotic regions with quasi-periodic windows in Fig. 3.

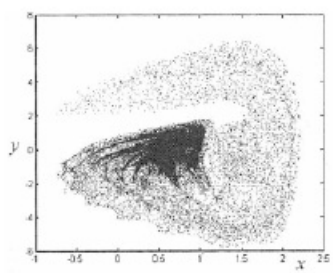

Figure 2: Poin*cáre* map for $f_1 = 6.1, \omega_1 = 1, f_2 = 0.75, \omega_2 = \sqrt{5}$.

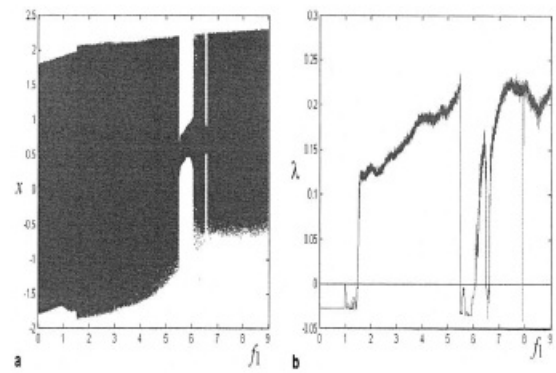

Figure 3: Bifurcation diagram and maximal Lyapunov exponents of the system (2) in (f_1, x) plane for $\omega_1 = 1, f_2 = 0.75, \omega_2 = \sqrt{5}$.

Case II : ω_1 is bifurcation parameter. Here are two sets of parameter values.

1. The Poin*cáre* map of the system (2) is shown in Fig. 4 for $f_1 = 30, \omega_1 = 2.2, f_2 = 2, \omega_2 = 2$ and it is chaotic attractor. The bifurcation diagram of the system (2) in (ω_1, x) plane for $f_1 = 30, f_2 = 2, \omega_2 = 2$, and the maximal Lyapunov exponents corresponding to the bifurcation diagram are shown in Fig. 5(a) and (b) respectively. We observe that quasi-periodic orbits and chaotic motion appear for $\omega_1 \in (0, 0.3)$ and chaotic behaviors and periodic motion appear alternately for $\omega_1 \in (0.3, 6)$.

2. The Poin*cáre* map of the system (2) is shown in Fig. 6 for $f_1 = 2, \omega_1 = 1.45, f_2 = 0.1, \omega_2 = \sqrt{5}$ and the system is in a chaotic state. The bifurcation diagram of the system (2) in (ω_1, x) plane for $f_1 = 2, f_2 = 0.1, \omega_2 = \sqrt{5}$ is shown in Fig. 7(a) and the maximal Lyapunov exponents corresponding to Fig. 7(a) are shown in Fig. 7(b). We show that quasi-periodic orbits and chaotic behaviors appear alternately.

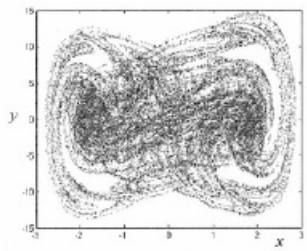

Figure 4: Poincáre map for $f_1 = 30, \omega_1 = 2.2, f_2 = 2, \omega_2 = 2$.

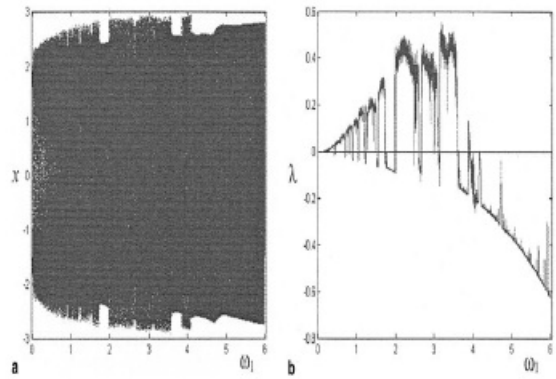

Figure 5: Bifurcation diagram and maximal Lyapunov exponents of the system (2) in (ω_1, x) plane for $f_1 = 30, f_2 = 2, \omega_2 = 2$.

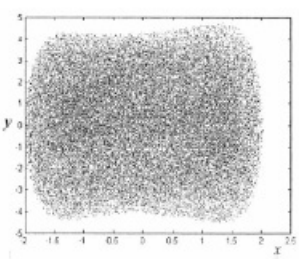

Figure 6: Poincáre map for $f_1 = 2, \omega_1 = 1.45, f_2 = 0.1, \omega_2 = \sqrt{5}$.

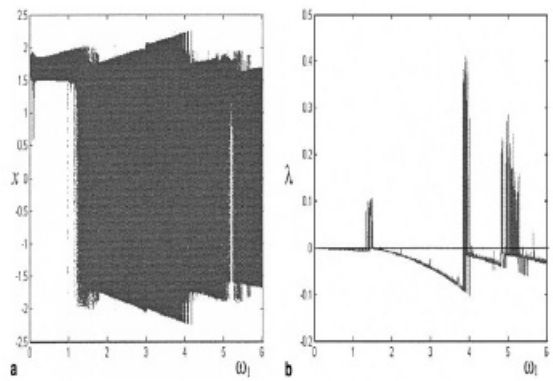

Figure 7: Bifurcation diagram and maximal Lyapunov exponents of the system (2) in (ω_1, x) plane for $f_1 = 2, \omega_1 = 1.45, \omega_2 = \sqrt{5}$.

3. Chaos Control of the System (2)

The above numerical results show that the system is in chaotic state for some parameters. In order to suppress and eliminate the chaotic behavior, it is necessary to control the chaos of the system (2). Here are two ways to solve this problem.

3.1 Variable Feedback Control

By using variable feedback control, the chaos of the system (2) is controlled. The original system's dynamical behaviors persist due to the change of small parameter has no effect

on the system. This method not only can stabilize the unstable periodic orbit in the original system, but also can create a new cycle of orbits.

By adding a feedback variable K (K is the adjustable feedback factor) to the first equation, the system (2) can be rewritten as

$$\begin{cases} \dot{x} = y - Kx, \\ \dot{y} = \mu(1-x^2)y - \omega_0^2 x - \lambda x^3 - \beta x^5 + f_1 \cos\omega_1 t + f_2 \cos\omega_2 t. \end{cases} \tag{4}$$

Even if the feedback coefficient is small, it can also significantly weaken the chaotic behavior, so the chaotic behavior of the system (2) can be inhibited by selecting the appropriate K.

For Case I, when $f_1 = 6.1, \omega_1 = 1, f_2 = 0.75$ and $\omega_2 = \sqrt{5}$, the system (2) is chaotic. Fixed the above data, the bifurcation diagram of the system (4) for $K \in (0, 1)$ is shown in Fig. 8(a). From Fig. 8(a) we can see the chaotic behavior has been effectively controlled by the feedback variable K. At the beginning of $K = 0$, the system (4) is in a very small chaotic region, namely, the chaotic motion of the system is in a narrow region, with K continuously increasing, near $K = 0.036036$ the chaotic state disappears, the system enter the quasi-periodic orbit, then the system is in wide area of quasi-periodic orbits. For clarity, the chaotic attractor for $K = 0.01$ and quasi-periodic orbits for $K = 0.2$ and $K = 0.9$ in phase portraits are shown in Fig. 8(b), (c) and (d) respectively. The chaotic attractor and invariant torus for $K = 0.01$ and $K = 0.2$ in Poin*cáre* map are given in Fig. 8(e) and (f), respectively.

For 1 of Case II, when $f_1 = 30, \omega_1 = 2.2, f_2 = 2$ and $\omega_2 = 2$, the system (2) is chaotic. The bifurcation diagram of system (4) for $K \in (0, 2)$ is shown in Fig. 9(a). We can see the chaotic area with quasi-periodic windows from Fig. 9(a). With K increasing from $K = 0$, the system (4) is in a wide chaotic region. When $0.66466 < K < 2$, the system (4) is in stable periodic orbits. The chaotic attractor for $K = 0.4$ and periodic orbits for $K = 0.7$ and $K = 1.8$ in phase portraits are shown in Fig. 9(b), (c) and (d) respectively. For clarity, the chaotic attractor for $K = 0.4$ and the periodic orbit for $K = 1.8$ in Poin*cáre* map are shown in Fig. 9(e) and (f), respectively.

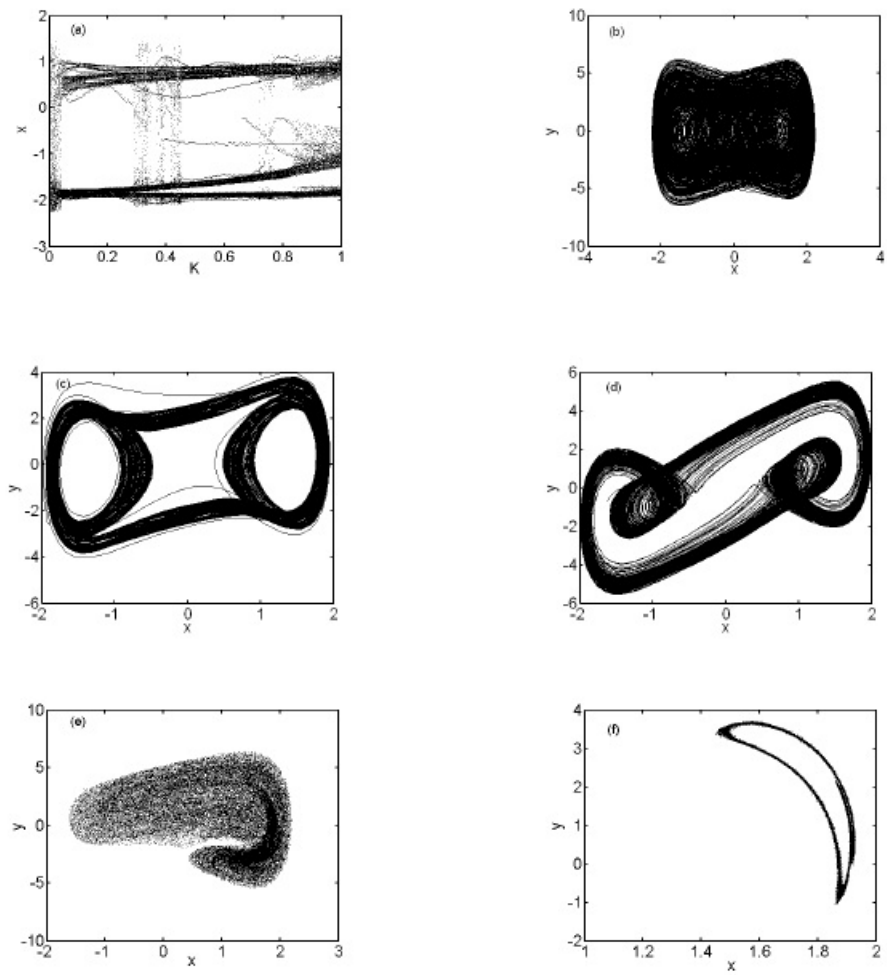

Figure 8 : (a) Bifurcation diagram of the system (4) in (K, x) plane for $f_1 = 6.1, \omega_1 = 1, f_2 = 0.75, \omega_2 = \sqrt{5}$. (b)(c)(d) Phase portraits for three values of K: (b) $K = 0.01$; (c) $K = 0.2$; (d) $K = 0.9$. (e) Poin*cáre* map of Fig. 8(b). (f) Poin*cáre* map of Fig. 8(c).

For 2 of Case II, system (2) is chaotic for $f_1 = 2, \omega_1 = 1.45, f_2 = 0.1$ and $\omega_2 = \sqrt{5}$. The bifurcation diagram of system (4) for $K \in (0, 1)$ is shown in Fig. 10(a). Near $K = 0.075075$, the system (4) is from the chaotic state into stable quasi-periodic orbits, and quasi-periodic orbits account for wide area. The Fig. 10(a) shows two different kinds of quasi-periodic orbits: one is in $0.075075 < K < 0.67768$ and the another is in $0.67768 < K < 1$. The very clear show of the chaos into quasi-periodic invariant circle can be seen from Fig. 10(a). The chaotic attractor for $K = 0.01$ and quasi-periodic

orbit for $K = 0.1$ and $K = 0.8$ in phase portraits are shown in Fig. 10(b), (c) and (d) respectively. For clarity, the chaotic attractor for $K = 0.01$, quasi-periodic orbits for $K = 0.1$ and $K = 0.4$, and the non-attracting chaotic set for $K = 0.8$ are given in Fig. 10(e)-(h).

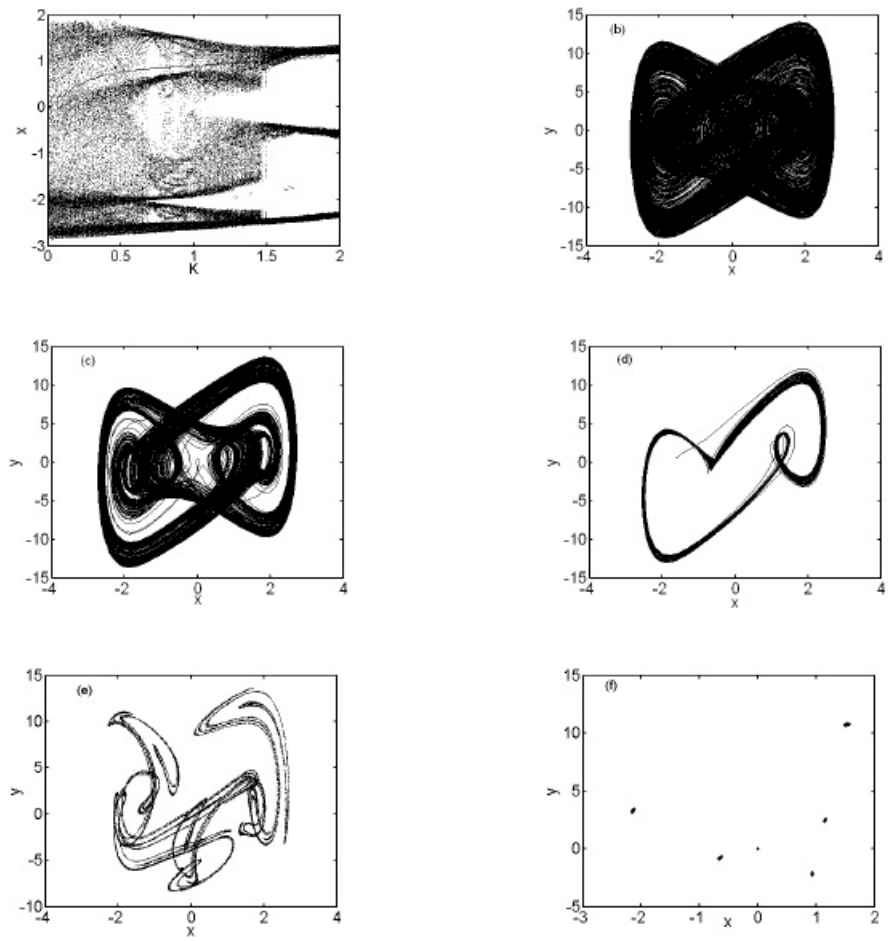

Figure 9 : (a) Bifurcation diagram of the system (4) in (K, x) plane for $f_1 = 30, \omega_1 = 2.2, f_2 = 2, \omega_2 = 2$. (b)(c)(d) Phase portraits for three values of K: (b) $K = 0.4$; (c) $K = 0.7$; (d) $K = 1.8$. (e) Poin*cáre* map of Fig. 9(b). (f) Poin*cáre* map of Fig. 9(d).

By numerical simulations (bifurcation diagrams, phase portraits and Poin*cáre* map of the system (4) under feedback variable K $(K > 0)$), chaos, generated by three sets of data in Section 2.2, is controlled respectively. By numerical simulations, it can be found

that variable feedback control method has good control effect, and the method is simple and easy to implement, without too much of the knowledge of the controlled system, and it control chaos stably and reliably.

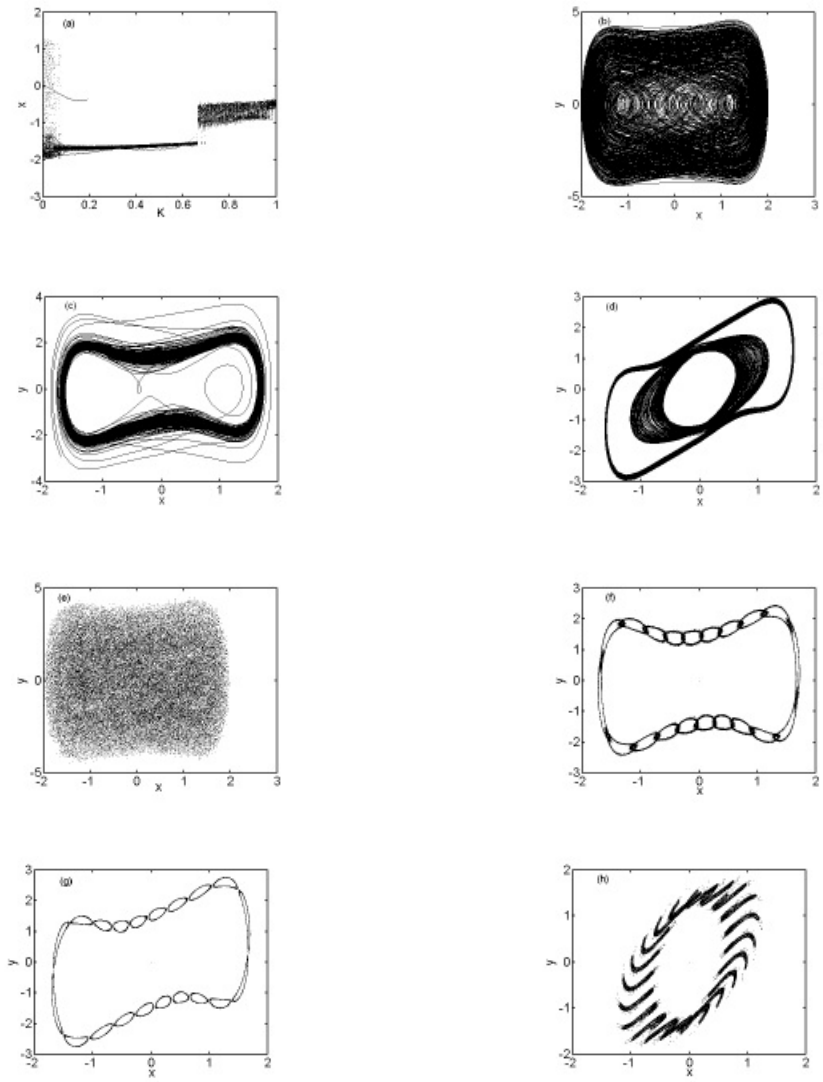

Figure 10 : (a) Bifurcation diagram of the system (4) in (K, x) plane for $f_1 = 2, \omega_1 = 1.45, f_2 = 0.1, \omega_2 = \sqrt{5}$. (b)(c)(d) Phase portraits for three values of K: (b) $K = 0.01$; (c) $K = 0.1$; (d) $K = 0.8$. (e) Poin*cáre* map of Fig. 10(b). (f) Poin*cáre* map of Fig. 10(c). (g) Poin*cáre* map of the system (4) for $K = 0.4$. (h) Poin*cáre* map of Fig. 10(d).

3.2 Coupled Feedback Control

With the control signal $f(t) = L[x(t) - y(t)]$ coupled with the periodic signal $y(t)$ and the output $x(t)$ of the system (1), where L is the weight for the control signal to adjust the intensity, so we can get the system (5)

$$\begin{cases} \dot{x} = y, \\ \dot{y} = \mu(1 - x^2)y - \omega_0^2 x - \lambda x^3 - \beta x^5 + f_1 \cos \omega_1 t + f_2 \cos \omega_2 t + L[x - y]. \end{cases} \tag{5}$$

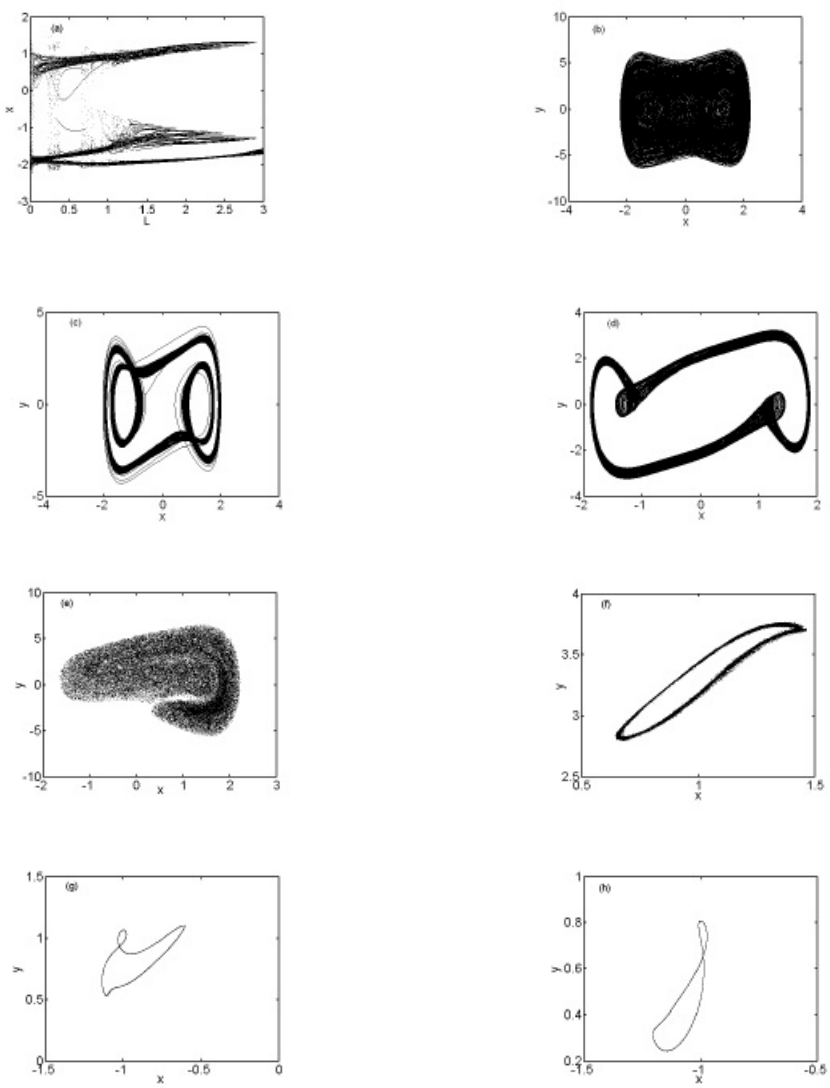

Figure 11 : (a) Bifurcation diagram of the system (5) in (L, x) plane for $f_1 = 6.1, \omega_1 = 1, f_2 = 0.75, \omega_2 = \sqrt{5}$. (b)(c)(d) Phase portraits for three values of L: (b) $L = 0.001$;

(c) $L = 0.5$; (d) $L = 2$. (e) Poin*cáre* map of Fig. 11(b). (f) Poin*cáre* map of Fig. 11(c). (g) Poin*cáre* map of Fig. 11(d). (h) Poin*cáre* map of the system (5) for $L = 3$.

The case as an example to Case I, the bifurcation diagram of the system (5) for $L \in (0, 3)$ is shown in Fig. 11(a). From Fig. 11(a) we can see the behaviors of the system (5) remain chaotic as L increases from zero. When L arrives at and pass through a critical value $L \approx 0.03003$, the behavior changes from chaotic to quasi-periodic, namely L suppresses chaos in the system (5). The phase portraits of different L ($L > 0$) in the system (5) are shown in Fig. 11(b), (c) and (d): (b) $L = 0.001$; (c) $L = 0.5$; (d) $L = 2$. For clarity, we give the chaotic attractor, the strange non-chaotic attractor and two invariant torus in Poin*cáre* map at $L = 0.001, L = 0.5, L = 2$ and $L = 3$ in Fig. 11(e)-(h) respectively.

4. Conclusion

By applying phase portraits, potential diagram, Poin*cáre* maps, bifurcation diagrams, maximal Lyapunov exponents, the chaotic behavior of the system (2) is studied qualitatively and quantitatively. By numerical simulations, the impact of excitation amplitude f_1 and the vibration frequency ω_1 on the system (2) is analyzed respectively. Using two kinds of control methods on the system (2), the chaotic state is controlled effectively. Different control methods have different advantages and can be required to choose.

Acknowledgement

This work is supported by the National Natural Science Foundation of China (Nos.11471197 and 11402139), Research Project Supported by Shanxi Scholarship Council of China (No.2013-019) and the Natural Science Foundation of Shanxi Province (No.2014011005-1). Corresponding author. E-mail address: hongyu@sxu.edu.cn (Y. Shi).

References

[1] Chu Y. D., Li X. F., Zhang J. G., Chaos contorlling and bifurcation of Van der Pol-Duffing system, Journal of Southern Yangtze University: Natural Science Edition, 6(1) (2007), 119-123. (in Chinese).

[2] Ge Z. M., Leu W. Y., Anti-control of chaos of two-degrees-of-freedom loudspeaker system and chaos synchronization of different order systems, Chaos, Solitons and Fractals, 20 (2004), 503-521.

[3] Guckenheimer J., Hoffman K., Weckesser W., The forced Van der Pol equation. I: The slow flow and its bifurcations, SIAM Journal on applied dynamical system, 2(1) (2003), 1-35.

[4] Hua C. C., Lu Q. S., A class of time-dependent bifurcation problem and the Duffing-Van der Pol oscillator, Mechanics and Engineering, 23(1) (2001), 24-26.

[5] Jing Z. J., Wang Q. R., Chaos in Duffing system with two external forcings, Chaos, Solitons and Fractals, 23 (2005), 399-411.

[6] Jing Z. J., Yang Z. Y., Jiang T., Complex dynamics in Duffing-Van der Pol equation, Chaos, Solitons and Fractals, 27 (2006), 722-747.

[7] Kakmeni F. M. M., Bowong S., Tchawoua C., Kaptouom E., Strange attractors and chaos control in a Duffing-Van der Pol oscillator with two external periodic forces, Journal of Sound and Vibration, 227 (2004), 783-799.

[8] Kao Y. H., Wang C. S., Analog study of bifurcation structures in a Van der Pol oscillator with a nonlinear restoring force, Physical Review E, 48 (1993), 2514-2520.

[9] Lakshmanan M., Murali M., Chaos in Nonlinear Oscillations, World Scientific, (1996).

[10] Leung A. Y. T., Zhang Q. L., Complex normal form for strongly non-linear vibration systems exemplified by Duffing-Van der Pol equation, Journal of Sound and Vibration, 213(5) (1998), 907-914.

[11] Li Q. H., Lu Q. S., Analysis of dynamical behaviors of a coupled Van der Pol-Duffing oscillator, Journal of Henan Normal University: Natural Science, 30(4) (2002) 15-18. (in Chinese).

[12] Liang Y., Namachchuraya N. S., P-bifurcation in the noise Duffing-Van der Pol equation, Springer, New York: Stochastic Dynamics, (1999), 49-70.

[13] NamachchiVaga N. S., Sowers R. B., Vdula L., Non-standard reduction of noisy Duffing Van der Pol equation, Journal of Dynamic Systems, 16(3) (2001), 223-245.

[14] Parlitz U., Lauterborn W., Period-doubling cascades and Peril's staircases of hte Driven Van der Pol oscillators, Physical Review A, 36 (1987), 1428-1434.

[15] Rajasikar S., Parthasarathy S., Lakshmanan M., Prediction of horseshoe chaos in BVP and DVP oscillators, Chaos, Solitons and Fractals, 2 (1992), 271-280.

[16] Wakako M., Chieko M., Koi-ichi H., Yoshi H. I., Integrable Duffing's maps and solutions of the Duffing eqaution, Chaos, Solitons and Fractals, 15(3) (2003), 425-443.

[17] Wang R. Q., Jing Z. J., Chaos control of chaotic pendulum system, Chaos, Solitons and Fractals, 21 (2004), 201-207.

[18] Wiggins S., Introduction to Applied Nonlinear Dynamical System and Chaos, New York, Springer-Verlag, (1990).

[19] Xu L., Lu M. W., Cao Q. J., Nonlinear dynamical bifurcation analysis of Van der Pol-Duffing equation, Chinese Journal of Applied Mechanics, 19(4) (2002), 130-133.

[20] Yagasaki K., Detection of bifurcation structures by higher-order averaging for Duffing's equation, Nonlinear Dynamics, 18 (1999), 121-158.

[21] Yagasaki K., Homoclinic tangles, phase locking, and chaos in a two frequency perturbation of Duffing's eqaution, Journal of Nonlinear Science, 9 (1999), 131-148.

[22] Zhang L., Yu J. N., Li Y., Peng J. K., Chaos control for the periodically excited Van der Pol-Duffing, Journal of Wenzhou University: Natural Sciences, 28(2) (2007), 11-14. (in Chinese).